

# Kinetic Optimization of a Protein-Responsive Aptamer Beacon

Bradley Hall,<sup>1</sup> Sean Cater,<sup>2</sup> Matt Levy,<sup>3</sup> Andrew D. Ellington<sup>1</sup>

<sup>1</sup>Department of Chemistry and Biochemistry, Institute for Cellular and Molecular Biology, University of Texas at Austin, Austin, Texas 78712; telephone: 512-471-6445; fax: 512-471-7014; e-mail: andy.ellington@mail.utexas.edu

<sup>2</sup>Bio-Rad Laboratories Headquarters, Hercules, California

<sup>3</sup>Department of Biochemistry, Albert Einstein College of Medicine, Bronx, New York

Received 25 September 2008; revision received 27 February 2009; accepted 3 April 2009

Published online 9 April 2009 in Wiley InterScience (www.interscience.wiley.com). DOI 10.1002/bit.22355

**ABSTRACT:** Aptamers have been utilized as biosensors because they can be readily adapted to sensor platforms and signal transduction schemes through both rational design and selection. One highly generalizable scheme for the generation of the so-called aptamer beacons involves denaturing the aptamer with antisense oligonucleotides. For example, rational design methods have been utilized to adapt anti-thrombin aptamers to function as biosensors by hybridizing an antisense oligonucleotide containing a quencher to the aptamer containing a fluorescent label. In the presence of thrombin, the binding equilibrium is shifted, the antisense oligonucleotide dissociates, and the beacon lights up. By changing the affinity of the antisense oligonucleotide for the aptamer beacon, it has proven possible to change the extent of activation of the beacon. More importantly, modulating interactions between the antisense oligonucleotide and the aptamer strongly influences the kinetics of activation. Comparisons across multiple, designed aptamer beacons indicate that there is a strong inverse correlation between the thermodynamics of hybridization and the speed of activation, a finding that should prove to be generally useful in the design of future biosensors. By pre-organizing the thrombin-binding quadruplex within the aptamer the speed of response can be greatly increased. By integrating these various interactions, we were ultimately able to design aptamer beacons that were activated by threefold within 1 min of the addition of thrombin.

Biotechnol. Bioeng. 2009;103: 1049–1059.

© 2009 Wiley Periodicals, Inc.

**KEYWORDS:** thrombin; aptamer beacon; signaling aptamer; kinetics; thermodynamics; biosensor

## Introduction

Aptamers have proven to be useful as biosensors, in large measure because they can be readily adapted to a variety of sensor platforms and signal transduction schemes through the rational manipulation of their sequences and secondary structures (Bunka and Stockley, 2006; Cho et al., 2008; Deisingh, 2006; Nutiu and Li, 2005). Aptamer beacons have been designed that function similarly to molecular beacons, in that interaction with analytes leads to a separation of fluorophore and quencher, and subsequent “light up” signaling. A general scheme for the design of aptamer beacons involves creating an antisense oligonucleotide that denatures the functional structure of an aptamer, and placing a fluorescent reporter and quencher so that they are in apposition to one another in the denatured structure (Nutiu and Li, 2003). Upon binding to a target analyte, the equilibrium between the antisense-bound, non-functional structure and the free functional structure will be altered, with a concomitant change in observed fluorescence. While this and other signal transduction schemes readily yield aptamer biosensors that can sensitively detect a variety of analytes, the kinetic properties of the resultant biosensors have not been examined in any detail.

We have therefore generated a series of aptamer beacons that can detect the protein thrombin, and examined their kinetics of signaling. While the anti-thrombin aptamer is generally chosen for biosensor development because of its simplicity, in this instance it was chosen in large measure because so many previous studies have utilized this aptamer. The single-stranded DNA aptamer is relatively short (15 nucleotides; 5'-GGTTGGTGTGGTTGG) and its structure is known in atomic detail by both NMR (Macaya et al., 1993; Schultze et al., 1994; Wang et al., 1993) and crystallography (Padmanabhan et al., 1993). The potassium-dependent aptamer forms a unimolecular quadruplex in solution in which two G-quartets are connected by two TT

Correspondence to: A.D. Ellington

Contract grant sponsor: National Institute of Biomedical Imaging and BioEngineering

Contract grant number: 5 R01 EB003424

Contract grant sponsor: Defense Advanced Research Projects Agency Tactic Grant

Contract grant number: Project # 183409J

loops and a TGT loop (Fig. 1A). This aptamer was found to bind to thrombin's fibrinogen recognition exosite (FRE) with a  $K_d$  of approximately 100 nM (Bock et al., 1992). However, it was later discovered that by incorporating a terminal helix of between four to seven base pairs, the binding affinity could be further increased between 4- and 10-fold (Macaya et al., 1995).

Another reason to utilize thrombin as a target for detailed studies of aptamer biosensors is that an additional, different anti-thrombin aptamer has been selected (60–18 with the sequence 5'-AGTCCGTGGTAGGGCAGGTTGGGGTGGACT-3'). This newer anti-thrombin aptamer also displays potassium-independent binding (Macaya et al., 1995; Tasset et al., 1997; Tsiang et al., 1995). While this aptamer again forms a G-quadruplex, the termini of the quadruplex forms a duplex that stabilizes the

structure and further improves its binding affinity (Fig. 1B). In contrast to the shorter quadruplex, however, the extended quadruplex was found through photo-crosslinking experiments to interact with a different epitope, the heparin-binding exosite.

Anti-thrombin aptamers have previously been extensively utilized for the development of biosensors. In 2001, Stanton and coworkers engineered the original anti-thrombin aptamer to act to form an alternative, hairpin structure (Hamaguchi et al., 2001). A fluor and quencher were included at the aptamer termini, leading to quenching in the absence of thrombin (Fig. 1C). Upon the addition of thrombin, though, the equilibrium was shifted in favor of the G-quadruplex, concomitantly separating the fluor from the quencher and leading to thrombin-dependent fluorescent signaling. The anti-thrombin aptamer was also

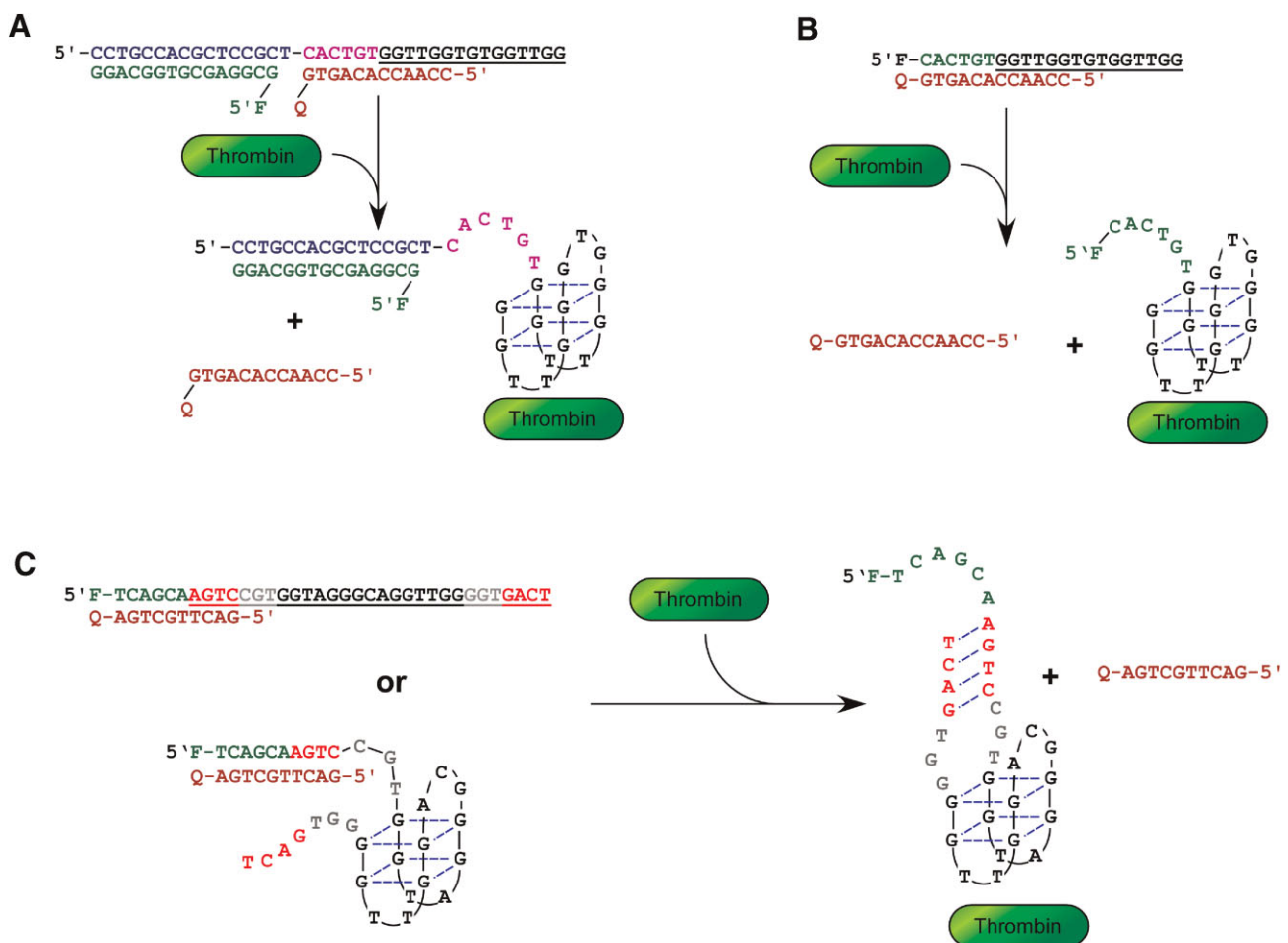


**Figure 1.** Structure switching models. Alternative conformations that are favored in the presence and absence of thrombin are shown. Different fonts and colors are used to allow the reader to better follow the conformational change. In general, the aptamer sequence is underlined, green is the sequence adjacent to the fluorescein, purple is the sequence adjacent to the quencher, red is the sequence that forms a duplex stem in the binding conformation, and gray is an internal bulge. (A) Structure-switching reporter developed by Nutiu with the original author's naming conventions in parentheses (2003). The underlined sequence is consensus anti-thrombin aptamer (Bock et al., 1992), later called G15D (Tasset et al. 1997). The oligonucleotide (FDNA1) is labeled with a 5'-Fluorescein and the oligonucleotide QDNA6 is labeled with a 3'-DABCYL. Additional sequences that assist in secondary structure formation in the non-binding conformer are shown in blue and purple. The G-quartet is drawn to represent the three-dimensional structural arrangement. (B) Representative activation of Apt4 (Stem-2) and Th.Q1 (QDNA6). (C) AptH complexed with Th.Q5-2. AptH is derived from 60 to 18 (underlined; Tasset et al. 1997) with TCAGCA appended to the 5' end.

engineered to function as an FRET beacon (Li et al., 2002). In this instance, the aptamer structure was destabilized in the absence of thrombin, and the addition of thrombin allowed terminal fluorophores to interact, thus changing the fluorescence spectra.

In an attempt to generalize the design of aptamer biosensors, Nutiu and Li (2003) developed both bipartite and tripartite aptamer beacons. In this case, the inactive conformer was formed by hybridization of one or more antisense oligonucleotides to the anti-thrombin aptamer, and displacement of the antisense oligonucleotide(s) led to signaling. The advantage of this method is that it is more modular: the antisense oligonucleotides can contain both fluorescent reporters and quenchers. The aptamer activated nearly instantaneously at 37°C, yet was considerably slower at lower temperatures. Finally, both the shorter and longer quadruplex anti-thrombin aptamers have been utilized in a clever proximity assay in which joint binding of the aptamers lead to a large change in FRET signal (Heyduk and Heyduk, 2005).

We have now optimized two different bipartite thrombin aptamer beacons to have fast activation rates at room temperature (25°C). In carrying out these optimizations, we have begun to develop both empirical and quantitative methods for controlling the kinetics of aptamer biosensors. In particular, we show that there is a trade-off between the extent of activation and the speed of response, and that this trade-off relies to a large extent on the thermodynamics of secondary structure formation.

## Materials and Methods

### Synthesis and Purification of Oligonucleotides

All materials were synthesized by conventional methodologies (Hall et al., 2007). Briefly, 5' 6-FAM moieties were introduced as phosphoramidites, while 3' quenchers were introduced on controlled pore glass (CPG) solid supports (Glen Research, Sterling, VA). The quenchers utilized were DABCYL (4-(4-dimethylaminophenylazo)benzoic acid), Eclipse Quencher, and Black Hole Quencher 1 (BHQ-1). After deprotection samples were lyophilized and purified by HPLC (Nutiu and Li, 2003) with the following changes: the column was an XTerra MS C18 Column with dimensions of 4.6 mm × 30 mm, and bead diameters of 2.5 μm. The two solvents were 0.1 M TEAA and 100% acetonitrile on a nonlinear gradient from 5% to 35% acetonitrile over 30 min at a flow rate of 3 mL/min. We collected 2/3 (width) of the main peak that showed absorption at both 260 and 495 nm. The purified DNA was lyophilized and resuspended in 100 μL diH<sub>2</sub>O. Oligonucleotide concentrations were determined by measuring UV absorbance at 260 nm on a Nanodrop ND-1000 (Wilmington, DE). Molar extinction coefficients were calculated using the IDT (Coralville, IA) SciTools OligoAnalyzer 3.1 (Cantor et al., 1970; Cavaluzzi and Borer, 2004).

### Kinetic Assays

Assays were performed with 100 nM fluorescent oligonucleotide and 200 nM quencher oligonucleotide in 50 μL reactions. We originally chose to utilize the signaling buffer of Nutiu and Li (2003): 20 mM Tris pH 8.3, 5 mM KCl, 1 mM MgCl<sub>2</sub> as opposed to either of the original selection buffers (Bock et al., 1992) 20 mM Tris pH 7.4, 140 mM NaCl, 5 mM KCl, 1 mM MgCl<sub>2</sub>, and 1 mM CaCl<sub>2</sub>; (Tasset et al., 1997) 50 mM Tris pH 7.5, 100 mM NaCl, and 1 mM MgCl<sub>2</sub>) because both tripartite and bipartite constructs had been reported to signal in these buffers. Aptamer beacons were generated by mixing the two oligonucleotides in signaling buffer, heating the sample to 90°C for 3 min, then cooling to 25°C at 0.2°C/s. Samples were further equilibrated at room temperature (26°C) for an additional 5–15 min. Assays were carried out in Corning 96-well black opaque ½ area well plates (Corning, NY). Maximum fluorescence values were determined in the absence of the quencher oligonucleotide. Aptamer beacons were initially assayed for protein-dependent activation in the presence or absence of 1 μM thrombin (Haematologic Technologies, Essex Junction, VT) on a BioTek Synergy HT (Winooski, VT) fluorescent plate reader at between 25.7 and 26.8°C with a gain of either 48 or 50, such that a buffer blank yielded a signal of 26 relative fluorescent units (RFU). There was a lag in sample reading of between 0 and 20 s after thrombin addition (time point 0). Rate constants were calculated from a nonlinear regression curve fit of the data using SigmaPlot V9 and the equation  $A = A_0 e^{-kt}$ , where  $k$  is the rate of activation,  $t$  is the time, and  $A$  (amplitude of the reaction) is the fluorescence. The time necessary to reach half maximal signal ( $t_{1/2} = \ln(2)/k$ ).

### Thermodynamic Modeling

The DINAmelt 2-state Hybridization Server powered by the UNAFold software package (<http://www.bioinfo.rpi.edu/applications/hybrid/hybrid2.php>) was utilized to predict melting profiles for each nucleic acid pair (Table I; Markham and Zuker, 2005). The predicted  $T_m$  listed in Table I corresponds to the “ $T_m$  (Conc)” or the temperature at which the concentration of double-stranded molecules is half the maximum value. To predict this  $T_m$ , the following parameters were modified from the default settings to better represent experimental conditions: Temperature range from 0 to 100°C; NA type: DNA; Initial concentrations of fluorescent oligonucleotides [ $A_0$ ]: 0.1 μM, quencher oligonucleotides [ $B_0$ ]: 0.2 μM; Salts: 10 mM Na<sup>+</sup>, 1 mM Mg<sup>++</sup>.

### Experimental Determinations of $T_m$

Melts were performed on an Applied Biosystems 7300 Real Time PCR System (Foster City, CA) in skirted 96-well PCR plates using the FAM channel (~520 nm). Assays were set up in a manner identical to the kinetic assays described above.

**Table 1.** Thermodynamic profiles for aptamer:quencher oligonucleotide pairs.

Name	Sequence <sup>a</sup>	Predicted $\Delta G^\circ$ (kcal/mol) <sup>b</sup>	Predicted $T_m$ (°C) <sup>c</sup>	Actual $T_m$ (°C) <sup>d</sup>	# bp with quencher	Fold Activation <sup>e</sup>	% Min, Max Fluorescence <sup>f</sup>	$t_{1/2}$ (min) <sup>g</sup>	Rate (min <sup>-1</sup> ) <sup>g</sup>
5F.Apt.4	<u>CAC TGTGGTGGTGTGGTITGG</u>								
Th.Q1	GTGACACCAACC	-14.6	44.1	45.6	12	1.18 ± 0.02 3.70 ± 0.14 <sup>h</sup>	9%, 15%; 14%, 64%	- >30	- <0.02
Th.Q1-1	GTGACACCAAC	-12.8	40.1	40.0	11	2.98 ± 0.09 2.45 ± 0.06 <sup>h</sup>	19%, 57%; 26%, 93%	21 ± 3 3.3 ± 0.4	0.034 ± 0.004 0.21 ± 0.03
Th.Q1-2	GTGACACCAA	-11.2	37.0	33.7	10	2.12 ± 0.04 1.15 ± 0.03 <sup>h</sup>	40%, 94%; 72%, 97%	3.6 ± 0.2	0.19 ± 0.01
Th.Q1-3	GTGACACCA	-9.9	31.1	29.3	9	1.56 ± 0.03 1.17 ± 0.03 <sup>h</sup>	72%, 95%; 82%, 97%	-	-
Th.Q8 (DabcyI)				38.5		4.23 ± 0.05	12%, 54%	14 ± 1	0.050 ± 0.002
Th.Q8 (Eclipse)		-12.7	39.3	38.8	10	4.62 ± 0.06	9%, 46%	18 ± 1	0.038 ± 0.001
Th.Q8 (BHQ)				40.9		4.14 ± 0.10	6%, 30%	>30	<0.02
5F.Apt.7	<u>ACTGTGGTGGTGGTGGTITGG</u>								
Th.Q1	GTGACACCAACC	-13.4	41.7	39.0	11	3.58 ± 0.17	17%, 53%	>30	<0.02
5F.Apt.8	<u>CTGTGGTGGTGGTGGTITGG</u>								
Th.Q1 (DabcyI)				33.5		2.26 ± 0.02	39%, 97%	3.3 ± 0.2	0.21 ± 0.01
Th.Q1 (Eclipse)		-12.1	37.3	35.8	10	7.67 ± 0.01	9%, 85%	9.3 ± 0.1	0.074 ± 0.001
Th.Q8 (DabcyI)				40.5		2.35 ± 0.01	28%, 66%	11 ± 1	0.065 ± 0.002
Th.Q8 (Eclipse)		-11.7	36.6	41.3	10	2.63 ± 0.04	19%, 51%	15 ± 1	0.046 ± 0.002
Th.Q8 (BHQ)				45.1		2.61 ± 0.06	11%, 29%	>30	<0.02
5F.Apt.H	<u>TCAGCAAGTCGGTGGTAGGGCAGGTGGGGTGACT</u>								
Th.Q5	AGTCGTTACAGC	-15.5	45.1	37.9	12	2.61 ± 0.06	18%, 49%	4.1 ± 0.5	0.17 ± 0.02
Th.Q5-1	AGTCGTTACAG	-12.9	42.2	42.7	11	1.99 ± 0.07	7%, 15%	-	-
Th.Q5-2	AGTCGTTACAG	-11.3	37.6	33.5	10	3.00 ± 0.05	17%, 64%	<1	>0.7
Th.Q3-1	GTCGTTACAGC	-14.6	43.6	46.3	11	1.55 ± 0.02	7%, 12%	-	-
Th.Q3-2	TCGTTACAGC	-12.7	41.0	38.5	10	3.42 ± 0.05	13%, 49%	6.8 ± 0.7	0.10 ± 0.01

All data taken at 26°C unless otherwise specified.

<sup>a</sup>Sequence: The various data are for the aptamer hybridized separately to each of the quencher oligonucleotides. The quencher sequences are shown offset to the aptamer sequences to indicate where hybridization should occur. All aptamer sequences are listed in 5' → 3' direction whereas quencher sequences are listed 3' → 5' to show complementarity.

<sup>b</sup>Predicted  $\Delta G^\circ$ : The  $\Delta G^\circ$  value was predicted using the DINAMelt 2-state Hybridization Server powered by the UNAFold software (<http://dinamelt.bioinfo.rpi.edu/twostate.php>) at 25°C with 10 mM NaCl and 1 mM MgCl<sub>2</sub>.

<sup>c</sup>Predicted  $T_m$ :  $T_m$  values were calculated utilizing the DINAMelt web server with the conditions listed in Materials and Methods.

<sup>d</sup>Actual  $T_m$ : Error in the actual  $T_m$  measurement is reported as the calculated standard error in the curve fit line and is less than ±0.1°C in all instances. Number of base pairs with quencher: length of the hybridized aptamer:quencher.

<sup>e</sup>Fold activation: F/Fo at 30 minutes. Error in the measured fold activation is reported as the standard deviation of measurements taken in triplicate.

<sup>f</sup>%Min, Max fluorescence: the relative fluorescence of the fluoresceinated oligonucleotide with and without the quencher. % minimum fluorescence can be converted to quenching efficiency by subtracting from 100% as done in Marras et al. (2002).

<sup>g</sup> $t_{1/2}$  and rate constants are only reported if the activation was over 2-fold and the R<sup>2</sup> value of the curve that fit the data was greater than 0.95 as calculated by SigmaPlot v9.0. Error values for  $t_{1/2}$  and rate constants are reported as the standard errors for curve fit lines through the average of measurements taken in triplicate.

<sup>h</sup>The lower set of numbers for 5F.Apt.4 when bound to Th.Q1 through Th.Q3 for columns % Min, Max Fluorescence,  $t_{1/2}$ , and Rate corresponds to data taken at 37°C.

Samples were heated to 95°C for 15 s, then cooled to 10°C. Temperature ramps were performed from 10 to 95°C at a rate of ~0.1°C/s, and fluorescence was read after each 1°C increase. Experiments were repeated in triplicate. Results were normalized to minimum and maximum fluorescence, and the melting temperature ( $T_m$ ) was calculated as the peak of a curve fit through the first derivative of the sigmoidal melt curve (Mergny and Lacroix, 2003).

## Results and Discussion

### Designing Aptamer Beacons That Signal the Presence of Thrombin

Nutiu and Li (2003) have previously generated antisense displacement aptamer beacons for the detection of thrombin. In this work, two antisense oligonucleotides containing fluorescent and quencher moieties were annealed to and thereby denatured a short, anti-thrombin DNA aptamer known to form a quadruplex structure (Clone 29; Bock et al., 1992). Kumar and Maiti (2004) have also shown that the anti-thrombin quadruplex can be refolded to a duplex under physiological conditions when an antisense oligonucleotide is present. Interaction with thrombin disfavors the tripartite, quenched complex and stabilizes the quadruplex structure, thus destabilizing the quencher oligonucleotide and yielding an increase in fluorescence (Fig. 1A). The Li group demonstrated that the beacon responded quickly ( $t_{1/2} = 1.2$  min) at 37°C, but was considerably slower at room temperature. Precisely because aptamer beacons couple conformational changes with signaling in a rational way, they may prove to be particularly useful as autonomous, reversible biosensors that continuously monitor for the presence of analytes. If so, it will be important to optimize their performance under ambient conditions.

We have now utilized this displacement model to design additional aptamer beacon constructs. However, we have altered the model so that the fluorescent label is incorporated directly at the 5' end of the aptamer. In this way, only one antisense oligonucleotide is utilized to form the quenched, bipartite complex, and the release of this single inhibitor results immediately in a fluorescent signal (Fig. 1B and C). Since the only design variables for the two-piece constructs are the number and position of base-pairs between the aptamer and the antisense quencher oligonucleotide their performance can be more readily predicted, engineered, and optimized.

### Optimizing Quencher Length for Responsivity at Room Temperature

In order to better understand how aptamer beacon signaling and kinetics might be optimized we attempted to develop a sensor that could be utilized conveniently at room

temperature in real-time. We first generated a series of aptamer beacons in which the number and positions of base-pairs between the antisense quencher oligonucleotide and the aptamer beacon were changed (Fig. 2A; Apt4). Apt4 was synthesized with a fluorescein at its 5' end and a series of increasingly shorter antisense oligonucleotides were synthesized with DABCYL at their 3' ends. Since the shorter quencher oligonucleotides should form less stable complexes we hypothesized that the constructs might activate more quickly at room temperature (although this was not a certainty, given that the relationship between thermodynamic stabilities and activation barriers is generally unknown). While the aptamer beacons would get faster, we might also expect an increase in the proportion of the aptamers that lacked a quencher oligonucleotide, and therefore an increase in the background (nonspecific) signal and a decrease in the observed fold-activation. The degree to which speed could be balanced with effector-dependent signal was an engineering issue that had not been previously approached in any detail.

The aptamer beacons were constructed by heating the oligonucleotides together then cooling them to room temperature; the initial fluorescent signals were stable prior to the addition of thrombin. Different beacons were

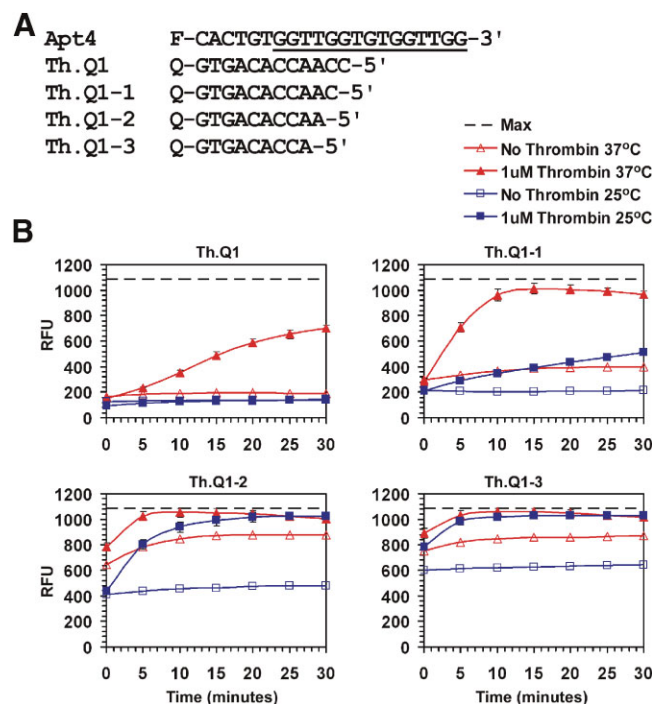


**Figure 2.** Activation of Apt4. **A:** Apt4 and quencher sequences. F denotes a fluorescein moiety, Q denotes a DABCYL moiety. **B:** Signal was measured in relative fluorescence units (RFU) over 30 min at 26 or 37°C in the absence (open marker) or presence of 1 μM thrombin (closed marker). Apt4 concentration was 100 nM while quencher oligonucleotides were 200 nM in 1× signaling buffer. The dashed black line represents Apt4 without quencher. Error bars represent standard deviation from triplicate samples.

quenched to different extents. The larger number of base-pairs gave lower backgrounds, with maximal quenching of fluorescence (nearly eightfold) observed for Th.Q1 at 26°C. Upon the addition of 1 μM (saturating) thrombin, fluorescence was monitored and the reaction was allowed to come to equilibrium over 30 min at either 26 or 37°C. As can be seen in Figure 2B, the smaller number of base-pairs generally gave larger final fluorescent signals.

By varying the extent of base-pairing and observing the resultant effects on background and signal, it proved possible to poise interactions between the anti-thrombin aptamer and its antisense quencher and thereby achieve particular extents and kinetics of activation. Th.Q1 is analogous to QDNA6 (Nutiu and Li, 2003), and showed 3.7-fold activation in our hands at 37°C after 30 min, but very little activation at 26°C. These results differed from those originally reported. Nutiu and Li (2003) found ~7-fold activation of the beacon in less than 3 min at 37°C, and ~8-fold activation at 25°C after 30 min. The difference in results may be due to the fact that our beacon is a two-piece rather than a three-piece construct. Our other two-piece designed beacons showed smaller activations: a 2.4-fold increase in signal over background was seen with Th.Q1-1 at 37°C, and a 3.0-fold increase with Th.Q1-2 at 26°C.

As the extent of activation decreased, the rate of activation increased, as predicted (Table I). Th.Q1-2 showed the fastest activation at room temperature ( $t_{1/2}$  = 3.6 min), while Th.Q1-1 showed the fastest overall activation ( $t_{1/2}$  = 3.3 min at 37°C). Th.Q1-3 showed too high a background to measure activation.

### Optimizing Aptamer Length for Responsivity at Room Temperature

Having found a two-piece aptamer beacon pair that was capable of activation within 30 min at room temperature, we began to modify other design variables to see what effects they might have on the extent and kinetics of activation. Instead of modifying the length of the antisense quencher oligonucleotide, we instead generated a number of shorter aptamer beacons (Apt6, Apt7, and Apt8; Fig. 3A). We assayed the new aptamer beacons with both the antisense quencher oligonucleotide Th.Q1, which was previously shown to fully quench, and Th.Q1-2, which provided the best activation and one of the best response times. As previously, decreasing the length and strength of hybridization led to greater background at room temperature (Fig. 3B). Th.Q1-2 did not quench either Apt7 or Apt8, nor was Th.Q1 capable of quenching an aptamer with a mismatch (data not shown).

Apt4 with Th.Q1-2 and Apt8 with Th.Q1 displayed similar activation rates at room temperature (Table I;  $t_{1/2}$  values of 3.6 and 3.3 min, respectively). The rough inverse correlation between extents and rates of activation was found to generally hold over numerous aptamer beacons (see also Fig. 6A). The fastest aptamer beacons were often those that formed stable but weak complexes, and thus were poised to be perturbed by the addition of ligand. Complexes that had a  $\Delta G^\circ$  value of ca. -11 to -12 kcal/mol led to improved kinetic performance. Indeed, there appeared to be quite steep kinetic cost to hybridization energies greater than -12 kcal/mol.

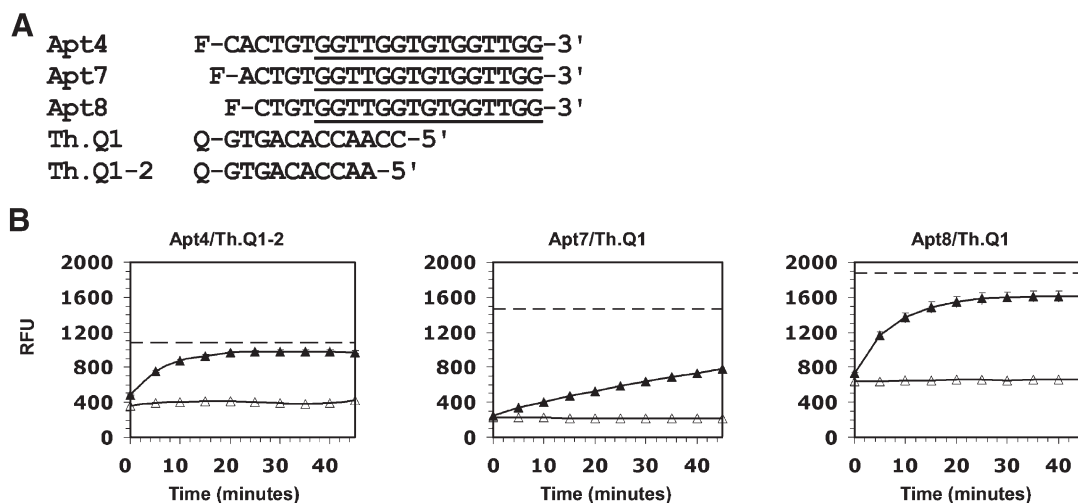


**Figure 3.** Effects of aptamer stem minimization. **A:** Aptamer and quencher sequences. F denotes a fluorescein moiety, Q denotes a DABCYL moiety. **B:** Signal was measured in RFU for Apt4 hybridized to Th.Q1-2, Apt7 hybridized to Th.Q1, and Apt8 hybridized to Th.Q1 over 30 min at 26°C in the absence (open marker) or presence of 1 μM thrombin (closed marker). Aptamer concentration was 100 nM while quencher oligonucleotides were 200 nM in 1× signaling buffer. The dashed black line represents maximum signal for each aptamer (in the absence of quencher). Error bars represent one standard deviation taken from triplicate samples.

## Effects of Quencher Type and Position on Aptamer Beacon Responsivities

Variable quenching efficiencies due to either contact quenching or FRET have previously been observed and measured with other hybridizing oligonucleotides (Dietrich et al., 2002; Marras et al., 2002). We therefore wanted to see whether quencher:fluor interactions also impacted the activation kinetics of our fastest aptamer beacons. We tested both Apt4 and Apt8 with two different antisense oligonucleotides, one which led to Q and F being in close proximity (Apt4/Th.Q1 or Apt8/Th.Q8) and another in which Q was separated by a two nucleotide spacer from F (Apt4/Th.Q8 or Apt8/Th.Q1; Fig. 4A). The Apt4/Th.Q1 complexes proved to be too stable, and did not activate at room temperature. For the other aptamer beacons, we also attempted to determine whether there were performance differences between commonly utilized quencher moieties, such as BHQ-1, DABCYL and Eclipse Quencher.

The extents of activation seen with the different quenchers were generally similar irrespective of the antisense quencher

oligonucleotide or aptamer beacon complex. The one exception was that aptamer beacons that displaced the quencher moieties away from the duplex (Apt 8/Th.Q1) had somewhat greater extents of activation. This may be because the quencher moieties had less chance to interact with the paired strands. This interpretation is consistent with previous findings, in that duplexes labeled with quenchers showed from 2 to 10°C greater melting temperatures compared with unlabeled duplexes (Marras et al., 2002).

Interestingly, quencher:strand interactions seem to affect kinetics much more strongly than activation. For example, when comparing Th.Q8 (quencher displaced) with Th.Q1 (quencher overlap) on Apt8, the extents of activation were almost all the same (Table I; 2.26% and 2.35%), yet the different quenchers yielded very different rates of activation (3.3 and 11 min<sup>-1</sup>). The aptamer beacons that incorporated DABCYL had two to three times faster responses, while those synthesized with BHQ-1 displayed the slowest responses (data not shown). Previous comparisons between these quenchers also showed that DABCYL had a lower impact on melting temperature of duplexes than BHQ-1

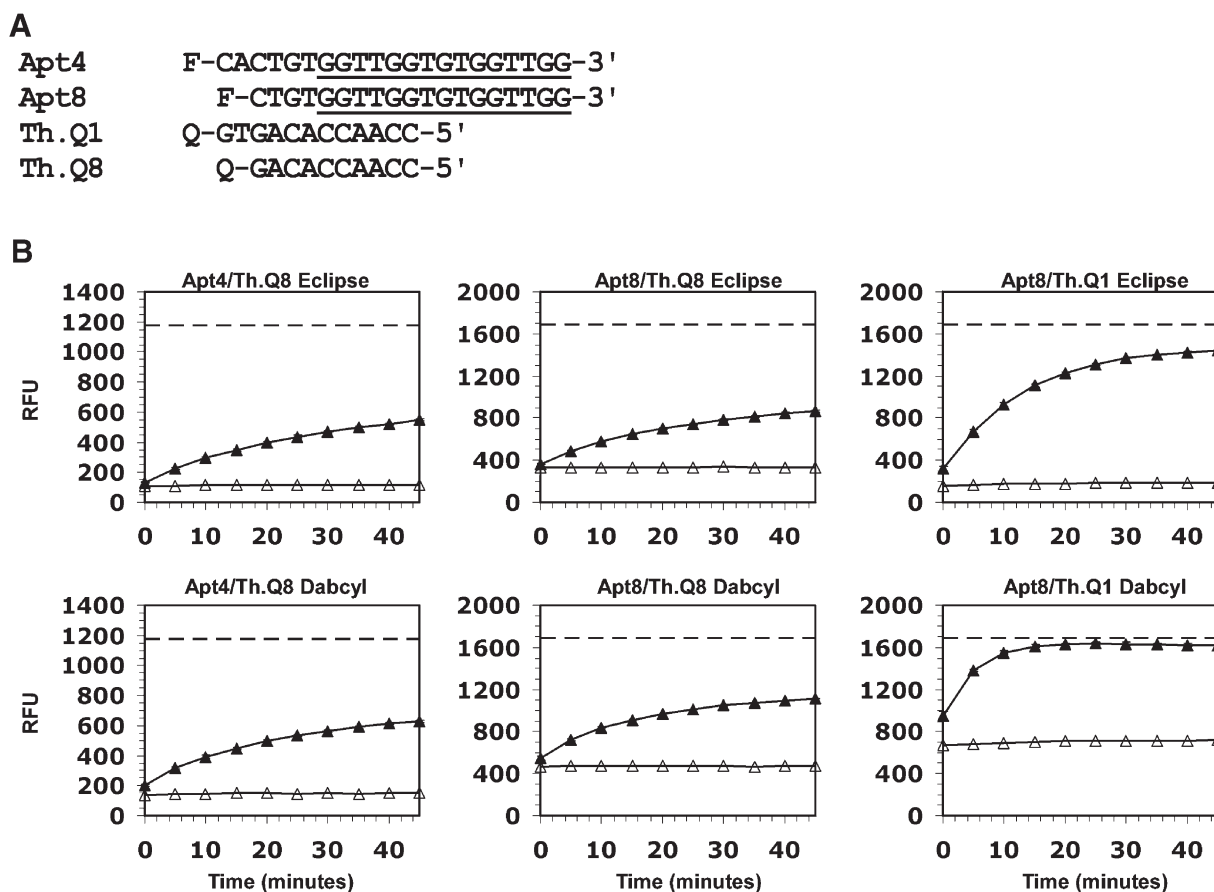


**Figure 4.** Varying quencher and position. **A:** Aptamer and quencher sequences. F denotes a fluorescein moiety, Q denotes either a DABCYL, or an Eclipse quencher. **B:** Signal was measured in RFU for Apt8 or Apt4 hybridized to either Th.Q1 or Th.Q8 quencher oligonucleotides with three different quencher moieties over 45 min at 26°C in the absence (open marker) or presence of 1 μM thrombin (closed marker). Aptamer concentration was 100 nM while quencher oligonucleotides were 200 nM in 1× signaling buffer. The dashed black line represents maximum signal for each aptamer (in the absence of quencher). Error bars represent one standard deviation taken from triplicate samples.

(Marras et al., 2002). It is possible that quencher interactions with the duplex not only stabilize the complexes but affect the “breathing” of the strands that may be necessary for faster switching between conformations.

### Designing Ligand Accessibility

Nutiu and Li (2003) also designed a tripartite aptamer beacon for sensing ATP, but found that their original design did not perform well at room temperature. They hypothesized that this was because the quencher oligonucleotide “occupied” the aptamer core sequence, presumably preventing nascent folding and ligand interactions. As a test of this hypothesis, they constructed a second ATP-sensing aptamer beacon with additional sequence at its 5' end, outside of the aptamer core. The extended binding site interacted with a quencher oligonucleotide with the same thermodynamic parameters as with the failed construct. However, this new construct yielded activation at room temperature with ATP.

We did not explicitly take into account an “occupation” parameter in our initial designs. However, in Apt8/Th.Q1 the antisense oligonucleotide occupies the core quadruplex much more than in Atp4/Th.Q1-2, yet the two aptamer beacons have similar activation extents and kinetics. However, it is interesting to note that the two aptamer beacons, Apt4/Th.Q1-2 and Apt8/Th.Q1, have the same overall number of base pairs, have predicted  $\Delta G$  values within 10% of each other, but Th.Q1 occupies the core quadruplex of Apt8 much more than Th.Q1-2 occupies Atp4. Nonetheless, these aptamer beacons have similar activation extents and kinetics, possibly indicating that pre-organization and occupation had little impact on kinetics. That said, the core quadruplex is occupied to some extent by the antisense quencher oligonucleotide in both beacons, so it may be that any interference with the core eliminates nascent binding.

Rather than merely extend previous constructs, we chose to utilize a known, functional anti-thrombin aptamer that was already extended beyond the core quadruplex structure. Tasset et al. (1997) had previously selected an anti-thrombin aptamer that once again formed a quadruplex structure, but also contained an extended stem (aptamer 60–18; Fig. 1C). Although the original (Bock et al., 1992) aptamer and the extended (Tasset et al., 1997) aptamer both form stacked G-quartets they contain different connecting loops and are thought to preferentially bind to different sites on thrombin. The Bock aptamer is thought to bind to thrombin’s fibrinogen recognition exosite, while the Tasset aptamer preferentially binds to the heparin exosite.

We designed two-piece aptamer beacons based on the Tasset aptamer. Since the additional base-pairs formed by the aptamer meant that the structure would be more difficult to denature, we utilized a series of antisense quencher oligonucleotides that hybridized with predicted  $\Delta G^\circ$  values of  $-11.3$  to  $-15.5$  kcal/mol (Fig. 1C; Table I).

While our previous constructs, above, allowed us to explore whether occupancy might be a factor in kinetic performance, we also utilized this new series of aptamer beacons to more explicitly test whether occupancy influenced kinetics. An additional six base “handle” (TCAGCA) was added at the 5' end; this moved the antisense quencher oligonucleotides completely outside of the quadruplex forming region of the aptamer (Figs. 1C and 5A). Whereas previously the antisense oligonucleotide interfered with quadruplex formation to different degrees, in these constructs the quadruplex should be able to form even with the antisense oligonucleotide bound.

As before, the least stable complexes (AptH/Th.Q3-2 and AptH/Th.Q5-2) gave the fastest activation (Fig. 5B). For the construct AptH/Th.Q5-2, full activation was detected within 30 s after addition of thrombin and before the first

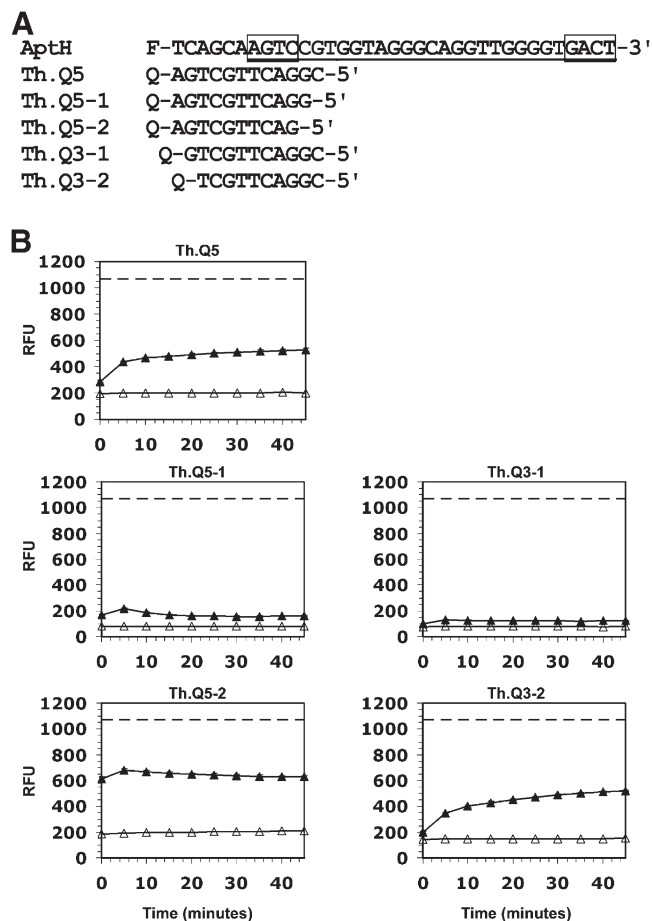


**Figure 5.** Aptamer Activation. **A:** Aptamer and quencher sequences. F denotes fluorescein moiety, Q denotes DABCYL moiety. The boxed sequence forms a duplex stem while the gray represents an internal bulge characteristic of this aptamer. **B:** Signal was measured in RFU for the sequences in (A) over 45 min at 26°C in the absence (open marker) or presence of 1 μM thrombin (closed marker). Aptamer concentration was 100 nM while quencher oligonucleotides were 200 nM in 1× signaling buffer. The dashed black line represents maximum signal for each aptamer (in the absence of quencher). Error bars represent one standard deviation taken from triplicate samples.

measurement by the microplate reader could be taken. These results were consistent with the hypothesis that nascent quadruplex formation greatly assisted in the kinetics of binding and response.

It should be noted that even when fully activated by protein these aptamer beacons showed only ca. 60% of the fluorescence seen in the absence of the quencher. We speculated that this might be because of protein-mediated quenching, but in the presence of protein and no quencher oligonucleotide the aptamer beacon showed full fluorescence, indicating that no significant quenching by protein had occurred. Thus, it seems possible that an equilibrium between bound protein and bound quencher has been established. This would be interesting because it may imply that these biosensors may have reversible performance.

More stable complexes (AptH/Th.Q3-1 and AptH/Th.Q5-1) gave little or no activation, with the exception of the most stable, AptH/Th.Q5. Interestingly, while AptH/Th.Q5 is predicted to be the most stable complex, it gave a higher background reading than the aptamer beacons that showed virtually no activation. We believe that AptH/Th.Q5 was not fully quenched in the absence of target due to a competition between binding to the aptamer and a fortuitous dimerization of the antisense quencher oligonucleotide to itself due to (resulting from a partial palindrome), and that this additional equilibria also led to the unexpected activation by thrombin.

Even though we predicted that a stronger interaction with the antisense quencher oligonucleotide would be necessary for aptamer beacon complex formation, it was again an antisense quencher oligonucleotide that bound with a  $\Delta G^\circ$  between  $-11$  and  $-12$  kcal/mol that gave the best performance (AptH/Th.Q5-2;  $-11.3$  kcal/mol). This aptamer beacon had remarkable kinetic responsivity, and was almost fully activated within 1 min.

### Predicting the Kinetics of Aptamer Beacons: Models and Caveats

The collection of data over multiple different aptamer beacon complexes provided an opportunity to try to generalize rules for aptamer beacon formation. Overall, for a given quencher complex there was an inverse correlation between the extent of activation ( $\ln[F/F_0]$ ) and the rates of activation, as previously noted (Fig. 6A; only DABCYL quenchers were plotted in order to avoid quencher-specific effects and AptH/Th.Q5-2 is discussed separately). There was also a strong inverse correlation between the speeds of response of aptamer beacons with a given quencher, and their stabilities as measured by melting temperatures of the antisense oligonucleotides containing DABCYL (Fig. 6B). This trend can of course be rationalized by suggesting that the antisense oligonucleotide must be released prior to forming the ligand-binding conformation and thus that the speeds of the various aptamer beacons were

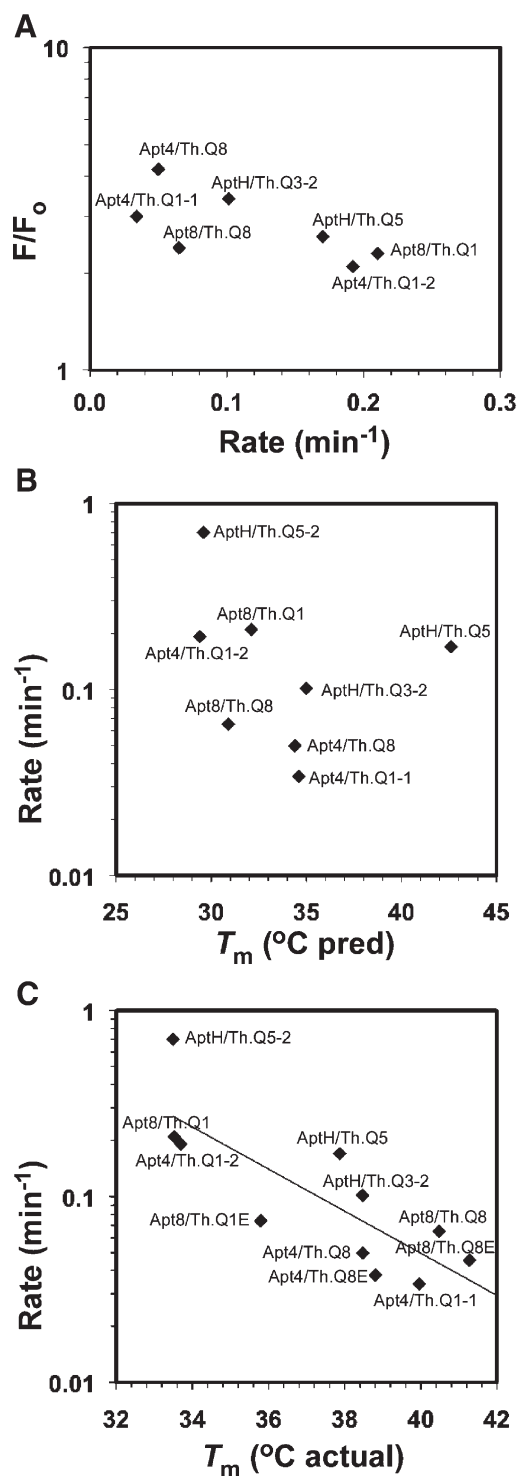


**Figure 6.** Comparison of thermodynamic and kinetic parameters from Table I for a subset of active aptamer beacons. In (A) we plot  $F/F_0$  on a log scale to emphasize the data trend. Only aptamers quenched with a DABCYL-labeled oligonucleotide were plotted in order to avoid quencher-specific effects and AptH/Th.Q5-2 is discussed separately. In (B) and (C) we plot rate on a log scale versus  $T_m$  because  $\ln(k_{-1}/k_1) = \Delta G_d/RT$ .  $\Delta G_d$  values should in turn be directly proportional to the enthalpies of dissociation, since the entropies of dissociation can be assumed to be roughly constant. In (C) the line fit corresponds to an  $R^2$  value of 0.65, fit to an exponential non-linear regression model with the equation  $y = 1666.4 \times e^{-0.261x}$ .

determined largely by the off-rates of the antisense quencher oligonucleotides.

This interpretation is also consistent with findings that quadruplex formation can be very fast. The quadruplex structural motif of the shorter thrombin binding aptamer is stabilized by ions such as potassium and magnesium (Hamaguchi et al., 2001; Tasset et al., 1997). Binding affinity and kinetic data have also been shown to be buffer, ionic strength, pH and temperature dependent (Bini et al., 2007; Hianik et al., 2007; Kumar and Maiti, 2004), and full activation can require from 10 s to hours. That said, the 15-mer FRE-binding anti-thrombin aptamer with fluorophores affixed to the terminal bases could switch within 10 s at 25°C in a physiological buffer that had a higher ionic strength and that contained sodium chloride (Li et al., 2002). Similarly, full activation was observed within 2 min in 20 mM Hepes pH 7.4, 10 mM KCl, 10 mM MgCl<sub>2</sub> and 0.2% Triton X-100 at room temperature when FRE-binding anti-thrombin aptamers were immobilized and monitored by surface plasmon resonance spectroscopy (Tang et al., 2007).

Given that the apparent stabilities of several of our aptamer beacon complexes differed from their predicted stabilities, based on both the observed background fluorescence and speeds of response, we decided to directly measure the  $T_m$  values of the aptamer beacons. To do this, beacons were prepared and the amount of free fluorescence was determined as a function of temperature from 10 to 95°C, with temperatures rising at a rate of ~0.1°C/s. A revised plot of measured  $T_m$  values versus rates showed a good congruence (Fig. 6C). These direct experimental measurements also allowed the inclusion of different quenchers in the same analysis. Overall, these results indicate that the kinetic responsivities of aptamer beacons can be largely predicted based on this single parameter.

That said, the extraordinary speed of AptH/Th.Q5-2 is inconsistent with a model in which kinetic control is due solely to antisense oligonucleotide dissociation. We hypothesize that this complex may pre-form a quadruplex structure that could interact with thrombin and speed the displacement of the antisense quencher oligonucleotide. A similar model has been proposed for the function of the so-called antiswitches (Bayer and Smolke, 2005), and is operative in nucleic acid logic circuits based on “toehold” sequences (Kim et al., 2006; Seelig et al., 2006). Interestingly, this aptamer beacon also has a relatively high  $F/F_0$  value, falling at the edge of the trend seen in Figure 6A. It may be that the simultaneous formation of the quadruplex and antisense duplex structures yields a low energy conformation that can only be activated (albeit quickly) by high protein concentrations, and we are further examining the mechanistic basis for the responsivity of this and other aptamer beacons.

We would like to thank Eun Jeong Cho for helpful discussions and her help with the design of Apt8. In addition, Shawn Piasecki helped with data collection for Figure 5. Brad Hall was partially supported by fellowships from Integrative Graduate Education and Research

Traineeship and the Freshman Research Initiative at the University of Texas at Austin. This work was funded by grants from National Institute of Biomedical Imaging and BioEngineering [5 R01 EB003424] and Defense Advanced Research Projects Agency Tactic Grant [Project # 183409J].

## References

- Bayer TS, Smolke CD. 2005. Programmable ligand-controlled riboregulators of eukaryotic gene expression. *Nat Biotechnol* 23(3): 337–343.
- Bini A, Minunni M, Tombelli S, Centi S, Mascini M. 2007. Analytical performances of aptamer-based sensing for thrombin detection. *Anal Chem* 79(7):3016–3019.
- Bock LC, Griffin LC, Latham JA, Vermaas EH, Toole JJ. 1992. Selection of single-stranded DNA molecules that bind and inhibit human thrombin. *Nature* 355(6360):564–566.
- Bunka DH, Stockley PG. 2006. Aptamers come of age—At last. *Nat Rev Microbiol* 4(8):588–596.
- Cantor CR, Warshaw MM, Shapiro H. 1970. Oligonucleotide interactions. 3. Circular dichroism studies of the conformation of deoxyoligonucleotides. *Biopolymers* 9(9):1059–1077.
- Cavaluzzi MJ, Borer PN. 2004. Revised UV extinction coefficients for nucleoside-5'-monophosphates and unpaired DNA and RNA. *Nucleic Acids Res* 32(1):e13.
- Cho EJ, Rajendran M, Ellington AD. 2008. Nucleic acids for reagentless biosensors. In: Ligler FS, Taitt CR, editors. *Optical biosensors*, 2nd edn: Today and tomorrow. Hungary: Elsevier. p 493–541.
- Deisingh AK. 2006. Aptamer-based biosensors: Biomedical applications. *Handb Exp Pharmacol* 173:341–357.
- Dietrich A, Buschmann V, Muller C, Sauer M. 2002. Fluorescence resonance energy transfer (FRET) and competing processes in donor-acceptor substituted DNA strands: A comparative study of ensemble and single-molecule data. *J Biotechnol* 82(3):211–231.
- Hall B, Hesselberth JR, Ellington AD. 2007. Computational selection of nucleic acid biosensors via a slip structure model. *Biosens Bioelectron* 22(9–10):1939–1947.
- Hamaguchi N, Ellington A, Stanton M. 2001. Aptamer beacons for the direct detection of proteins. *Anal Biochem* 294(2):126–131.
- Heyduk E, Heyduk T. 2005. Nucleic acid-based fluorescence sensors for detecting proteins. *Anal Chem* 77(4):1147–1156.
- Hianik T, Ostatna V, Sonlajtnerova M, Grman I. 2007. Influence of ionic strength, pH and aptamer configuration for binding affinity to thrombin. *Bioelectrochemistry* 70(1):127–133.
- Kim J, White KS, Winfree E. 2006. Construction of an in vitro bistable circuit from synthetic transcriptional switches. *Mol Syst Biol* 2:68.
- Kumar N, Maiti S. 2004. Quadruplex to Watson-Crick duplex transition of the thrombin binding aptamer: A fluorescence resonance energy transfer study. *Biochem Biophys Res Commun* 319(3):759–767.
- Li JJ, Fang X, Tan W. 2002. Molecular aptamer beacons for real-time protein recognition. *Biochem Biophys Res Commun* 292(1):31–40.
- Macaya RF, Schultze P, Smith FW, Roe JA, Feigon J. 1993. Thrombin-binding DNA aptamer forms a unimolecular quadruplex structure in solution. *Proc Natl Acad Sci USA* 90(8):3745–3749.
- Macaya RF, Waldron JA, Beutel BA, Gao H, Joesten ME, Yang M, Patel R, Bertelsen AH, Cook AF. 1995. Structural and functional characterization of potent antithrombotic oligonucleotides possessing both quadruplex and duplex motifs. *Biochemistry* 34(13):4478–4492.
- Markham NR, Zuker M. 2005. DINAMelt web server for nucleic acid melting prediction. *Nucleic Acids Res* 33: (Web Server Issue):W577–W581.
- Marras SA, Kramer FR, Tyagi S. 2002. Efficiencies of fluorescence resonance energy transfer and contact-mediated quenching in oligonucleotide probes. *Nucleic Acids Res* 30(21):e122.
- Mergny JL, Lacroix L. 2003. Analysis of thermal melting curves. *Oligonucleotides* 13(6):515–537.

- Nutiu R, Li Y. 2003. Structure-switching signaling aptamers. *J Am Chem Soc* 125(16):4771–4778.
- Nutiu R, Li Y. 2005. Aptamers with fluorescence-signaling properties. *Methods* 37(1):16–25.
- Padmanabhan K, Padmanabhan KP, Ferrara JD, Sadler JE, Tulinsky A. 1993. The structure of alpha-thrombin inhibited by a 15-mer single-stranded DNA aptamer. *J Biol Chem* 268(24):17651–17654.
- Schultze P, Macaya RF, Feigon J. 1994. Three-dimensional solution structure of the thrombin-binding DNA aptamer d(GGTTGGTG-TGGTTG). *J Mol Biol* 235(5):1532–1547.
- Seelig G, Soloveichik D, Zhang DY, Winfree E. 2006. Enzyme-free nucleic acid logic circuits. *Science* 314(5805):1585–1588.
- Tang Q, Su X, Loh KP. 2007. Surface plasmon resonance spectroscopy study of interfacial binding of thrombin to antithrombin DNA aptamers. *J Colloid Interface Sci* 315(1):99–106.
- Tasset DM, Kubik MF, Steiner W. 1997. Oligonucleotide inhibitors of human thrombin that bind distinct epitopes. *J Mol Biol* 272(5):688–698.
- Tsiang M, Jain AK, Dunn KE, Rojas ME, Leung LL, Gibbs CS. 1995. Functional mapping of the surface residues of human thrombin. *J Biol Chem* 270(28):16854–16863.
- Wang KY, McCurdy S, Shea RG, Swaminathan S, Bolton PH. 1993. A DNA aptamer which binds to and inhibits thrombin exhibits a new structural motif for DNA. *Biochemistry* 32(8):1899–1904.